POLİTEKNİK DERGİSİ

JOURNAL of POLYTECHNIC

ISSN: 1302-0900 (PRINT), ISSN: 2147-9429 (ONLINE)

URL: http://dergipark.org.tr/politeknik

CNN based determination of polycystic ovarian syndrome using automatic follicle detection methods

Otomatik folikül saptama yöntemleri kullanılarak ESA tabanlı polikistik over sendromu tespiti

Authors:, *Perihan Gülşah GÜLHAN[1] Güzin ÖZMEN[2], Hüsnü ALPTEKİN[3]*

ORCID[1]: 0000-0001-6749-332X

ORCID[2]: 0000-0003-3007-5807

ORCID[3]: 0000-0003-0851-9002

To cite to this article: Gülhan P. G., Özmen G ve Alptekin H., "CNN based determination of Polycystic Ovarian Syndrome using automatic follicle detection methods **"** ***Journal of Polytechnic***, 27(4): 1589-1601, (2024).

Bu makaleye şu şekilde atıfta bulunabilirsiniz: Gülhan P. G., Özmen G. ve Alptekin H., "CNN based determination of Polycystic Ovarian Syndrome using automatic follicle detection methods, **Politeknik Dergisi**, 27(4): 1589-1601, (2024).

Erişim linki (To link to this article): http://dergipark.org.tr/politeknik/archive

DOI: 10.2339/politeknik.1263520

CNN Based Determination of Polycystic Ovarian Syndrome Using Automatic Follicle Detection Methods

Highlights

- *A combined filter and threshold method was proposed for the detection of follicles and pcos in ultrasound images of the ovaries.*
- *It detects follicles using image processinf methods by comparing different filter and threshold combinations.*
- *CNN, with 18 layers, has been used to classify ovaries.*
- *The combination of the Wiener filter and adaptive threshold provided the best detection result*

Graphical Abstract

This study consists of two parts, follicle detection, and classification. First, the follicles were detected by image processing methods, and then the ovaries were classified as "normal" and "pcos".

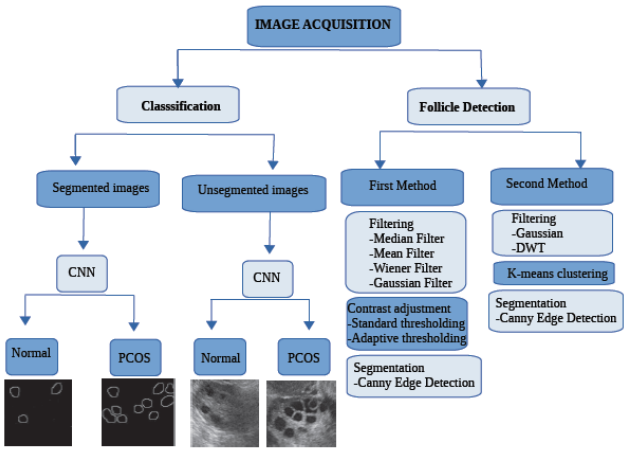

Figure. The flow diagram of this study

Aim

The aim of this study is to determine the best method for follicle detection using ovarian ultrasound images and classify the ultrasound images as pcos or normal ovary using proposed CNN architecture.

Design & Methodology

Two different methods for follicle detection were proposed to evaluate pcos. For this purpose, the median, the Average, the Wiener, and the Gaussian filter were tested with a standard and an adaptive threshold. Secondly, the Gaussian filtering, the Discrete Wavelet Transform, and the k-means clustering algorithm were tested. The Canny operator separated the follicles from the background in the segmentation phase.

Originality

In this study, the CNN architecture that classifies the limited ultrasound ovary image was developed and its success in the best follicle detection method was presented.

Findings

The highest follicle detection accuracy of 97.63% was achieved with adaptive thresholding using the Wiener resulting in 33.45% FAR and 1.6% FRR. The ultrasound images of the ovaries were classified as "normal" or "Polycystic ovary syndrome" using CNN architecture with classification accuracy of 65.81% for unsegmented ovarian images and 77.81% for segmented images. Classification success of transfer learning was 74.18%.

Conclusion

The results show that the combination of the Wiener filter with adaptive thresholding was quite successful in follicle detection and that CNN can better classify ovaries using preprocessed ultrasound images.

Declaration of Ethical Standards

The authors of this article declare that the materials and methods used in this study do not require ethical committee permission and/or legal-special permission.

CNN Based Determination of Polycystic Ovarian Syndrome using Automatic Follicle Detection Methods

Araştırma Makalesi/Research Article

Perihan Gülşah GÜLHAN[1], Güzin ÖZMEN[2], Hüsnü ALPTEKİN[3]

[1]Department of Electrical and Electronics Engineering, Institute of Sciences, Selcuk University, Turkey
[2] Department of Biomedical Engineering, Faculty of Technology ,Selcuk University, Turkey
[3]Department of Medicine, Medicana Hospital, Turkey

(Geliş/Received : 10.03.2023 ; Kabul/Accepted : 28.07.2023 ; Erken Görünüm/Early View : 11.09.2023)

ABSTRACT

The aim of this study was to determine the best method for follicle detection using ovarian ultrasound images and to classify the ultrasound images as pcos or normal ovaries using the proposed CNN architecture. Two different methods for follicle detection have been proposed to evaluate pcos. For this purpose, the Median, the Mean, the Wiener, and the Gaussian filters were tested using standard and adaptive thresholds. Second, Gaussian filtering, Discrete Wavelet Transform, and k-means clustering algorithms were tested. The Canny operator separates follicles from the background in the segmentation phase. In this study, a CNN architecture that classifies limited ultrasound ovary images was developed, and its success in the best follicle detection method was presented. The highest follicle detection accuracy of 97.63% was achieved with adaptive thresholding using a Wiener filter. Besides, the ultrasound images of the ovaries were classified as "normal" or "polycystic ovary syndrome" using CNN architecture with classification accuracy of 65.81% for unsegmented ovarian images and 77.81% for segmented images. In addition to the proposed method, classification was performed using SqueezeNet-based transfer learning, which was successful in limited datasets, and 74.18% classification accuracy was achieved for the unsegmented images and 75.54 % for segmented images . The results show that the combination of the Wiener filter with adaptive thresholding was quite successful in follicle detection and that the CNN can better classify ovaries using preprocessed ultrasound images.

Keywords: Automatic follicle detection, classification, convolutional neural networks, image preprocessing, ultrasound image, transfer learning.

Otomatik Folikül Saptama Yöntemleri Kullanılarak ESA Tabanlı Polikistik Over Sendromu Tespiti

ÖZ

Bu çalışmanın amacı, yumurtalık ultrason görüntülerini kullanarak folikül tespiti için en iyi yöntemi belirlemek ve önerilen CNN mimarisini kullanarak ultrason görüntülerini pkos veya normal yumurtalık olarak sınıflandırmaktır. Pkos'u değerlendirmek için folikül tespitinde iki farklı yöntem önerilmiştir. Bu amaçla Ortanca, Ortalama, Wiener ve Gauss filtresi; standart ve uyarlanabilir eşikle test edilmiştir. İkinci olarak, Gauss filtreleme, Ayrık Dalgacık Dönüşümü ve k-means kümeleme algoritması test edilmiştir. Segmentasyon aşamasında folikülleri arka plandan ayırmak için Canny operatörü kullanılmıştır. Bu çalışmada sınırlı ultrason over görüntüsünü sınıflandıran CNN mimarisi geliştirilmiş ve mimarinin optimum folikül tespit yöntemindeki başarısı sunulmuştur. Wiener Filtresi kullanılarak uyarlanabilir eşikleme ile %97.63' lük en yüksek folikül tespit doğruluğu elde edilmiştir. Ayrıca CNN mimarisi kullanılarak yumurtalıkların ultrason görüntüleri "normal" veya "polikistik over sendromu" olarak segmente edilmemiş over görüntüleri için %65,81 ve segmente edilmiş görüntüler için %77.81 sınıflandırma doğruluğu sınıflandırılmıştır. Önerilen yöntemin yanı sıra, sınırlı veri kümesinde oldukça başarılı olan SqueezeNet tabanlı transfer öğrenme kullanılarak sınıflandırma yapıldı ve segmente edilmemiş görüntüler için %74,18, segmente edilmiş görüntüler için %75.54 sınıflama doğrulupu elde edildi. Sonuçlar, Wiener filtresinin uyarlamalı eşikleme ile kombinasyonunun folikül tespitinde oldukça başarılı olduğunu ve CNN'nin önceden işlenmiş ultrason görüntülerini kullanarak yumurtalıkları daha iyi sınıflandırabildiğini göstermektedir.

Anahtar Kelimeler: Otomatik folikül tespiti, sınıflandırma, konvolüsyonel sinir ağları, görüntü ön işleme, transfer öğrenme, ultrason görüntüsü.

1. INTRODUCTION

Ovaries are divided into three groups according to their structural features: normal, cystic, and polycystic ovaries [1]. In normal ovaries, cysts containing eggs occur each month [2]. Each cyst that occurs in the ovaries is filled with water and expelled from the ovary with menstrual bleeding. Cysts that cannot be removed from the body remain in ovarian tissue and form polycystic ovaries. Although there are many follicles in polycystic ovaries, the follicles cannot mature and ovulation cannot occur. This is the main difference between polycystic and normal ovaries [3]. Polycystic ovary syndrome (PCOS) is a hormonal disorder that is characterized by various symptoms. It is found in nearly 20% of women of reproductive age [4]. According to the Rotterdam criteria, there are three basic criterions for the diagnosis

* *Corresponding Author*
e-mail: gozmen@selcuk.edu.tr

of PCOS [5], [6]. One of them is chronic anovulation, that is, menstrual irregularity; the second is excessive anrojenic hormones in women; and the third is the detection of follicles on ultrasound images. Women with at least two of these symptoms were considered to have PCOS [5]. To make a definitive diagnosis of this disease, the patient should be evaluated with a blood test.

PCOS causes many diseases that affect human life, such as diabetes, insulin resistance, obesity, and heart disease. For this reason, it is very important to diagnose this disease early and start treatment as soon as possible to prevent other diseases that will accompany it. The main symptoms of PCOS are insulin resistance and high luteinizing hormone (LH) levels, which induce ovulation in women. [4], [7], [8]. If PCOS remains untreated, it is associated with advanced diabetes and cardiovascular disease [8], [9]. Ultrasonography (USG) is a medical imaging method that uses sound waves at very high frequencies [12]. With USG, medical images are obtained in black and white colors in two dimensions. This imaging method is frequently used to determine PCOS. Ultrasound devices are used in the pre-diagnosis of many diseases, such as gallbladder diseases, breast tumors, and thyroid gland, prostate, and genital region diseases.

Ultrasound images of polycystic and normal ovaries are so different that they can be distinguished from each other. Normal ovaries have a maximum of 8-10 follicles, and with a diameter of these follicles–2-28 mm [10]. Patients with polycystic ovaries had 12 or more cysts in their ovaries. The diameter of these cysts was less than 9 mm [11]. For the ovary to be called a polycystic ovary, the ultrasound image must have more than 12 cysts, 2-9 mm in diameter [12]. The size of the cysts in the ovaries and the number of cysts were determined by ultrasound examination by the physician. Manual determination of follicles by experts is a time-consuming task. Therefore, the characteristics of the follicles are determined automatically, saving time for the physician and reducing the workload. Image processing involves the modification of digital images through various processes for purposes such as enhancement, storage, and recognition in the computer environment. When the studies on PCOS in the literature are examined, it has been seen that there are studies that detect follicles with different image processing methods [13].

There are several studies in the literature on follicle detection and classification. Lawrence et al., proposed a new method that automatically detects polycystic ovarian syndrome. They tested many segmentation methods and stated that the highest follicle recognition accuracy was obtained using the regional expansion algorithm, with 78% accuracy. They used mean and standard deviation features. They tested a Linear Discriminating Classifier (LDC), K-Nearest Neighbor (KNN), and Support Vector Machine (SVM). They achieved 92.86% accuracy, with the highest classification accuracy using LDC [13]. Hiremath and Tegnoo used a Gaussian low-pass filter and Contourlet Transform for noise filtering of ultrasound images of the ovaries. After denoising, histogram thresholding is performed. For edge detection, they used the Canny, Sobel, and Prewitt edge detection algorithms, and Canny achieved the best results for edge detection and segmentation. For evaluation, they compared the results with experts' decisions. They obtained classification accuracies of 62.3% with a Gaussian low-pass filter and 75.2% with a Contourlet Transform [14]. Purnama et al., developed a method to classify polycystic ovarian syndrome by using Gabor wavelet. For this purpose, they used the mean, entropy, kurtosis, skewness, and variance of the follicles. They classified the ovaries as "polycystic ovary" and "non-polycystic ovary" using normal and polycystic ovary images. Three different classification methods were used. As a result, classification accuracy was obtained with SVM-RBF kernel C=40 value of 82.55% in database A and 78.81% with KNN-euclidean distance K=5 value in database B [15]. Wisesty and Mutiah classified images using a Support Vector Machine (SVM) by extracting features from ultrasound images using the Gabor wavelet method. In their studies, the kernel function C=160, which provides the highest accuracy, was determined using the features obtained from the Gabor Wavelet result. They achieved classification accuracies of 78.46% and 75.54% for the test and training results, respectively [16]. Padmapriya et al. obtained the highest accuracy in automatic follicle identification in 2016 using morphological operations and the Canny edge detection operator, with a recognition rate of 87.5% [17]. Sonigo et al., presented an automated system for the determination of ovarian primordial follicle (PMF) numbers in mice. The classifier design was inspired by the VGG 19 architecture. A database was created by obtaining 9 million images from mouse ovaries. Using these images, the network was trained and tested with 3 million images. The accuracy of follicle detection was determined using true positive (TP) and false positive (FP) values. Approximately 89% of the follicles detected were FP. A precision of 11.32% and a recall of 99.46% were achieved. After hard negative mining HNM) application, 90.40% recall was obtained with 57.38% precision, and approximately 43% of the detected follicles were FP. The results improved, and a recall of 91.36% was obtained with 65.69% sensitivity. Approximately 19.5% of the

detected follicles are FP [18]. Nazarudin et al.. evaluated their performance by examining the methods used in previous studies on image segmentation. Watershed transform, regional amplification, edge-based, active contour, thresholding, and clustering methods were compared for image segmentation [19]. Zeng and Liu, worked on the follicle images of cattle. They mentioned that the basic image detection algorithm does not provide good results owing to speckle noise and follicles with blurred edges in the images; therefore, they proposed a method of detecting follicles with deep learning. They classified them using the Faster R-CNN model they developed and the classical model and compared the results. While the success rate of the classic Faster R-CNN was 75.4%, the success rate of the developed Faster R-CNN was 78.3% [20]. Rao and Kumar performed follicle detection using an adaptive k-means clustering algorithm for ultrasound image segmentation. The proposed method was tested on images that were divided into three classes: "normal ovary", "cystic ovary", and "polycystic ovary". The mean square error (MSE) of the normal and adaptive clustering methods was 95.8% and the MSE of adaptive clustering is 94.5%, respectively. The adaptive clustering algorithm yielded better results than other methods [21]. İnik et al., designed two separate CNN architectures for segmentation and classification to be used in the detection of follicles. For this purpose, they divided the subimages into three groups: margin, follicle, and background. They also proposed a new method to remove noise after segmentation and determine the border of the follicles, and they performed data augmentation for classification. They achieved a success rate of 95.35% using their proposed method [22]. Rachana et al., proposed a follicle recognition algorithm in the detection of polycystic ovary syndrome. Histogram thresholding and various morphological operations were applied to the images and Otsu thresholding was used for segmentation. The proposed method provides classification with 97% accuracy using a KNN classifier [23].

This study consisted of two parts, follicle detection and classification. First, the follicles were detected by image processing methods, and then the ovaries were classified as "normal" and "pcos." Determining the number and size of ovarian follicles is a laborious and time-consuming process. This study aims to use image processing and Convolutional Neural Networks (CNN) to accelerate follicle detection. For this purpose, 54 ovarian ultrasound images were obtained from the public data set. Various image processing techniques have been applied to ovarian ultrasound images to reduce noise and interference and equalize contrast imbalances. Two methods have been proposed for this purpose. In the first method, 4 different filter operations were tested. These are the median, mean, Gaussian, and Wiener filters. Morphological operations of erosion, opening, and dilation were applied to the images. The results of standard thresholding and adaptive thresholding used for contrast adjustment were then compared. In the second method, noise filters of Gaussian filter and Discrete Wavelet Transform are compared. After six different clusters were applied to the images using the k-means clustering algorithm, various morphological procedures were applied sequentially for follicle detection. In both methods, the follicles were separated from the background using the Canny operator during the segmentation stage. The success of follicle detection in the two methods was evaluated using the false acceptance rate (FAR) and false rejection rate (FRR). The method that provided the best detection was then determined. After follicle detection, a new dataset was created by recording segmented images. Another application of this study was to classify the ovaries as "normal ovarian" and "polycystic ovarian" using the CNN deep learning architecture. For this purpose, the number of unsegmented images was increased by applying rotation, horizontal reflection, vertical projection, and histogram equalization methods to a limited number of ovarian images for classification. The same process was applied to the segmented images, and the amount of data was increased by five times, and a total of 270 images, 200 normal ovarian images, and 70 PCOS images were obtained. Although data augmentation has been performed using various methods, the amount of data is insufficient. The classification was performed using the Squeezenet-based Transfer Learning method, which is very successful in low datasets and is compared with the proposed method.

2. MATERIAL AND METHOD

Fig. 1 presents a flow diagram of the methods used for follicle detection and classification in this study.

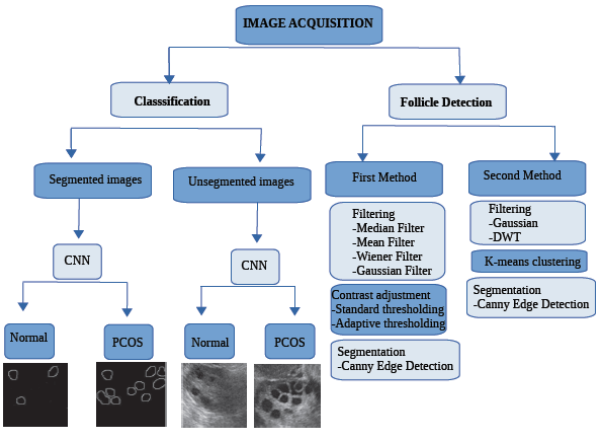

Fig. 1. The flow diagram of this study

2.1. Image Acquisition

The dataset used in this study was derived from Telkom University's public website. Ultrasound images of 14 patients with PCO and the 40-control subject were obtained using an ultrasound device with a vertical probe, prepared with expert opinion. All images were in JPG format with a size of 200 × 200 × 3, and there were 54 images in total [24].

2.2. Follicle Detection

To enhance the ultrasound images and minimize the noise, preprocessing of the image is required. In this way, unimportant details were removed, and important regions were highlighted. In this study, two different methods were used for the pre-processing stage [25].

For automatic follicle detection, an application was designed in MATLAB GUI that includes filtering and thresholding algorithms. The designed application is presented in Figure 2.

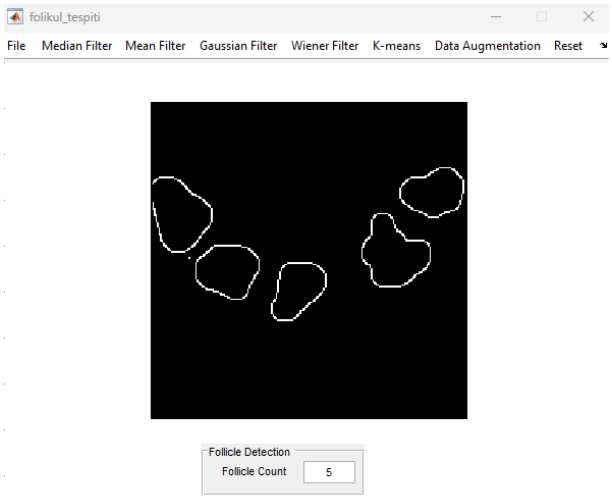

Fig. 2. An automated MATLAB GUI application is designed for filtering and thresholding

2.2.1. Image pre-processing

Images are exposed to various noises during digitization and are transferred from the camera to the computer. This noise causes deterioration in the image quality. Images were passed through various filters for noise reduction and image enhancement [26]. Filtering is often used to highlight certain parts of an image, soften the image, and remove unnecessary noise. Calculations become more complex and time-consuming as the size of the filters increases.

In this study, Mean, Median, Gaussian, and Wiener Filters were used for the first method. The Mean Filter structure is simple and easy to implement. Typically, a 3 × 3 matrix is used. It is used in a 5 × 5 matrix to provide additional smoothing in the image [26]. Because the Mean Filter takes the average of all nearby pixels, it causes sharp edges to soften and the image to change. However, significant differences in the images are destroyed, which is a disadvantage. A Median filter is developed to eliminate this problem. The Median Filter provides noise reduction and less loss of detail in the image [27]. This filter works slower than the mean filter [28]. In this study, a 3 × 3 matrix was used for the median filter, which had nine gray values when sorted in ascending order. In this case, the median value was the fifth value. The Wiener Filter aims to minimize the mean of the squares of error (MSE). This generates an estimated output signal based on the input signal. It filters the corrupted signal by separating the noise from the known signal. The Gaussian filter is very successful in preserving edge sharpness while removing white noise. This is achieved by convolving the image with a Gaussian kernel, which effectively smoothens the noise while maintaining the sharpness of the edges.

2.2.2. Contrast adjustment

The contrast is the difference between the brightest and darkest parts of the image. The greater the difference, the better is the image. In this study, two contrast adjustment methods, histogram equalization and adaptive thresholding, were applied after filtering. Histogram equalization was first applied to the filtered image to compensate for contrast inequalities. The histogram of an image is a graph formed by the grey values of the pixels of the image. The histogram chart provides information about the image. If the image has low contrast, its histogram is narrow. If an image does not have too much detail, histogram equalization is performed to refine the image. In particular, if the image is dark, the details are often not clear, and in this case, it is necessary to diffuse the gray levels of the pixels. With histogram equalization,

the gray levels in the image are uniformly distributed [29]. The gray levels in an image range from g_{min} to g_{max}. $G - 1 > g_{max} - g_{min}$, the desired gray level to be spread over the interval [0, G − 1] is calculated using the following equation: The process of spreading gray values is called histogram thresholding (HT). Equation (1) represents the gray-level spreading [30], where g_{new} is the brightness value obtained as a result of the process, g_{old} is the original brightness value of the image, g_{min} is the minimum pixel value in the image, g_{max} is the maximum pixel value in the image, and G is the maximum value that the brightness value can take.

$$g_{new} = \left(\frac{g_{old} - g_{min}}{g_{max} - g_{min}}\right) * G \quad (1)$$

2.2.3. Morphological operation

Morphological processes are image-processing techniques that utilize the structure of objects and regions to distinguish objects [31]. Morphological operations include dilation, erosion, opening, and closing, and are usually applied to black-and-white images [32]. Dilation fills the gaps by enlarging the object in the image, whereas erosion reduces the objects in the image [26]. If there are connected objects in the image, erosion and openings shrink and separate from each other. When the image is first dilated and then eroded, this process is called an opening. In the opening process, noise and unnecessary elements in the image are reduced or removed. If the image is first eroded and then dilated, the process is called closing. In the closing process, the gaps between the objects in the image are filled [26].

2.2.4. Discrete Wavelet Transform

The Discrete Wavelet Transform (DWT) was used to parse data in image processing [33]. Because the images contain discrete values, DWT was used instead of the Continuous Wavelet Transform. Ultrasound images contain a lot of noise, and DWT removes this noise. For the DWT, component separation is performed on grayscale images using the luminance parameter, and these components are then processed. Images were decomposed into subspaces using the coefficients for the DWT. A single-level transformation of a 2-Dimensional (2-D) DWT is presented in Fig.3.

An F(x,y) image of M×N dimensions is filtered by the x dimension. g(x) denotes high pass filter and h(x) denotes low pass filter. As a result of the transformation, the approximate coefficients are named $F_{LL}(x,y)$, horizontal details $F_{LH}(x,y)$, vertical coefficients $F_{HL}(x,y)$, and diagonal coefficients $F_{HH}(x,y)$ [35].

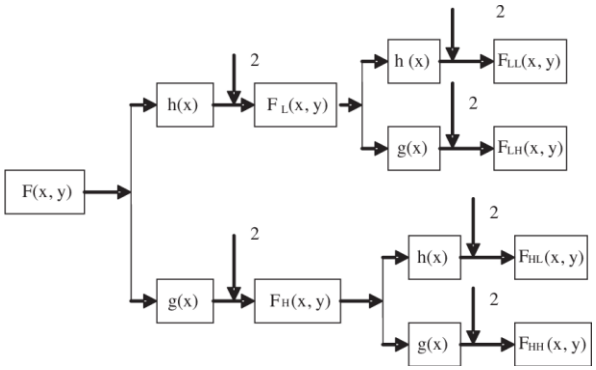

Fig. 3. Single level decomposition of 2-D DWT [35]

The size of the input images used in this study was 200×200 pixels. By applying 2-D DWT, the images were divided into four components: approximation coefficients, horizontal detail coefficients, vertical detail coefficients, and diagonal detail coefficients. The stages after decomposition were continued using the approximation coefficient component. After the DWT conversion, the image size decreased to 100 × 100. The image was resized and doubled to return to its original size.

2.2.5. K-means clustering algorithm

The K-means clustering algorithm separates similar points group by group, according to the determined center point. According to these groups, the desired operations were performed more effectively. The k-value in the k-means clustering algorithm determines the number of clusters and is included in the calculations as a parameter [36]. The K-means algorithm attempts to detect k clusters that will make the squared error the smallest. In this study, k was determined as 6. The important point here is that the values in the clusters should be similar to each other, but the clusters should be as different as possible. One of the obtained clusters was selected and the segmentation process was continued [37].

2.2.6. Segmentation

With segmentation, the boundaries and areas of the objects in an image are determined, while the object and background in the image are separated from each other. Consequently, similar regions in the image were separated from the other regions. Segmentation also provides information regarding the edges, corners, areas, and colors of the objects in the image. The main criterion for image segmentation in gray-level images is brightness. In color images, the main criterion is the color component [29]. The segmentation process is performed using many different methods, such as edge detection and

thresholding. Segmentation based on edge detection is performed using edge detection-based operators such as Canny, Sobel, and Prewitt [38]. In this study, the Canny edge detection algorithm, which is the most preferred edge detection operator for ultrasound images, was used.

2.3. Classification model and evaluation

2.3.1. Classification with CNN

Similar to many other fields, Deep Learning algorithms are used to classify USG images. Objects in images are labelled and classified using various decision-making mechanisms, such as artificial intelligence algorithms. Machine learning or deep learning can be used for classification. Deep-learning algorithms are constantly used in image processing, classification, segmentation, regression, and identification. Deep Learning was chosen for classification in this study because deep learning has the advantage of classifying objects with high performance without requiring feature extraction. Deep Learning determined features, such as the size and shape of the follicle, and those with similar features were placed in the same class. Deep Learning uses multiple layers between the input and output, with nonlinear processing units[39]. Deep Learning is able to analyze large amounts of data using multiple layers. The layers between the input and output perform feature identification so that feature extraction is not required again. Therefore, Deep Learning is advantageous because manually extracting features and learning the network requires a long time. However, the learned features can be easily adapted and learned quickly. The general structure of convolutional neural networks (CNN), which is a commonly used deep learning network for image classification, is shown in Fig. 4.

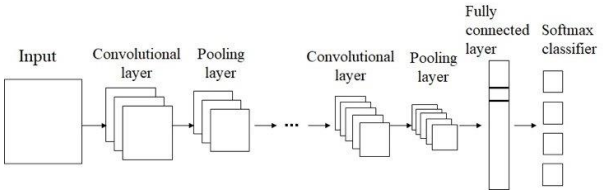

Fig. 4. The structure of CNN [40]

Classification using deep learning is an up-to-date and open-to-development process recently preferred in the medical field. To obtain better results in deep learning applications, large datasets are required, and it is difficult to collect these data. Therefore, the input images are reproduced using methods such as rotation, rescaling, mirroring, histogram equalization, translation, and noise addition. In this study, rotation, horizontal and vertical projections, and histogram equalization were used for data augmentation. Thus, five times more data were obtained than the images we obtained, and the total number of input images was 270. Fig. 5 shows a few examples of data augmented by rotation, horizontal mirroring, vertical mirroring, and histogram equalization methods.

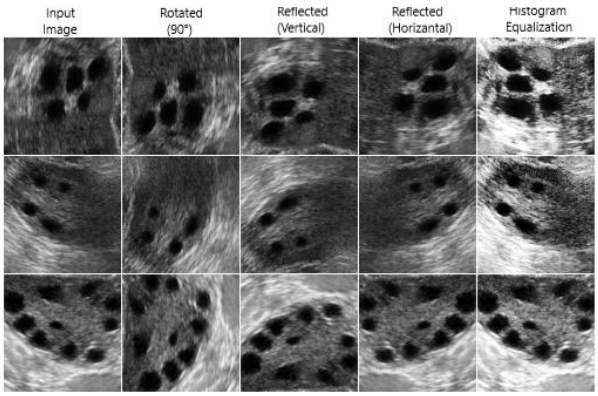

Fig. 5. Data augmentation with rotation, horizontal mirroring, vertical mirroring, and histogram equalization

In this study, unsegmented (raw) and segmented images were classified using CNN architecture. In the classification of the segmented images, the location and number of follicles were determined. The dataset was then divided into training, validation, and testing datasets. The layers created for the CNN were adjusted according to the size of the image using the equation (W−F+2P)/S+1. Here, W defines the size of the input image, and is accepted as 200×200. The number of steps (S) was set to one for the convolution layer and two for the pooling layer, and the P-value was set to zero. For the C1 layer, an 11 × 11 filter was applied; for the C2, C3, and C4 layers, a 10 × 10 filter was applied; and for the C5 layer, a 4 × 4 filter was applied. A 2 × 2 filter was used for layers P1, P2, P3, and P4. As a result of these processes, the input size was obtained as 1x1. Table 1 and Fig.6. show the features of the network layers.

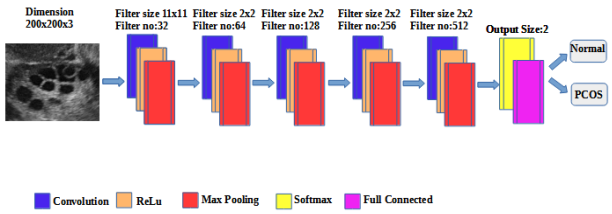

Fig. 6. Proposed CNN architecture with details layered view

Table 1. Properties of CNN's layers

Layer Numbers	Layer Name	Layer Properties
1	Input Layer	200x200x3
2	Convolution Layer (C1)	Filter: 11x11
3	ReLu Layer	
4	Pooling Layer (P1)	Filter: 2x2
5	Convolution Layer (C2)	Filter: 10x10
6	ReLu Layer	
7	Pooling Layer (P2)	Filter: 2x2
8	Convolution Layer (C3)	Filter: 10x10
9	ReLu Layer	
10	Pooling Layer (P3)	Filter: 2x2
11	Convolution Layer (C4)	Filter: 10x10
12	ReLu Layer	
13	Pooling Layer (P4)	Filter: 2x2
14	Convolution Layer (C5)	Filter: 4x4
15	ReLu Layer	
16	Fully Connected Layer	Output size: 2
17	Softmax Layer	
18	Classification Layer	

After the layers were set, the training options were determined and the network was trained. The training was started using stochastic gradient descent with momentum (sgdm), the learning rate was set to 0.01, and the maximum number of iterations for training was set to 32. The learning rate was determined by a trial-and-error method. The network was trained by considering the validation and test data, and classification accuracies were compared. Table 2. presents the CNN training options for classification.

Table 2. CNN's training options

Training options	SGDM
Initial Learn Rate	0.01
Max Epochs	32
Validation Data	imdsValidation
Validation Frequency	30
Verbose	False
Execution Environment	CPU

2.3.2. Classification with Transfer Learning

Transfer learning uses the knowledge gained from training the model in one task to execute it more efficiently on another task, or to achieve better results using less data. An insufficient amount and irregularity of data are significant problems for the classifier. In these cases, a solution can be provided using Transfer Learning with pretrained parameters. Transfer learning is an alternative method for small datasets [41]. In this study, SqueezeNet-based Transfer Learning is used. Unlike the others in the Squeeze Net architecture, the last layer is the convolution layer. This layer was updated according to the dataset and classification was performed. The input layer was also updated according to the input size.

Table 3. Transfer Learning's training options

Training options	SGDM
Initial Learn Rate	0.0001
Max Epochs	8
Validation Data	imdsValidation
Validation Frequency	5
Verbose	False
Execution Environment	CPU

Table 4. Properties of SqueezeNet's layers

Layer Numbers	Layer Name	Layer Properties
1	Input Layer	200x200x3
2	Conv1 {Conv+ReLu}	Filter: 3x3 Output:113x113x64
3	Pool1{Max Pool}	Filter: 3x3 Output:56x56x64
4	Fire2{Squeeze+ReLu -Expand+ReLu Concat}	Output:56x56x128
5	Fire3{Squeeze+ReLu -Expand+ReLu Concat}	Output:56x56x128
6	Pool3{Max Pool}	Filter: 3x3 Output:28x28x128
7	Fire4{Squeeze+ReLu -Expand+ReLu Concat}	Output:28x28x256
8	Fire5{Squeeze+ReLu -Expand+ReLu Concat}	Output:56x56x128
9	Pool5 {Max Pool}	Filter: 3x3 Output:14x14x256
10	Fire6{Squeeze+ReLu -Expand+ReLu Concat}	Output:14x14x384
11	Fire7{Squeeze+ReLu -Expand+ReLu Concat}	Output:14x14x384
12	Fire8{Squeeze+ReLu -Expand+ReLu Concat}	Output:14x14x512
13	Fire9{Squeeze+ReLu -Expand+ReLu Concat}	Output:14x14x512
14	Conv10 {Conv+ReLu}	Filter: 1x1 Output:14x14x3
15	Pool10 {Average Pool}	Output:1x1x3
16	Fully Connected Layer	Output:1x1x3
17	Softmax Layer	Output:1x1x3
18	Classification Layer	

3. PERFORMANCE EVALUATION METRICS

3.1. Evaluation metrics for the filters

The performance of the filters used for image processing was evaluated using Mean Square Error (MSE) and peak

signal-to-noise ratio (PSNR) metrics. For calculation, the original and enhanced images were normalized using min–max normalization. The lower the MSE value, the greater is the similarity between the two images. MSE was calculated by using Equation (2) where M×N is the matrix size of the image, I is the original image, and K is the noisy image.

$$MSE = \frac{1}{MxN}\sum_{i=0}^{m-1}\sum_{j=0}^{n-1}[I(i,j) - K(i,j)]^2 \quad (2)$$

PSNR is used to measure image quality in filtering applications [42]. The higher the PSNR value, the better the image quality. In a well-filtered image, it is desirable to have a low MSE and high PSNR. Equation (3) presents the PSNR calculation, where MAX_I is the maximum value of a pixel in the image.

$$PSNR = 10\log_{10}(\frac{MAX_1^2}{MSE}) \quad (3)$$

3.2. Evaluation metrics for the follicle detection

False Acceptance Rate (FAR) and False Rejection Rate (FRR) metrics were used to evaluate the follicle detection performance. FAR is where non-follicular areas are defined as follicles. On the other hand, FRR areas with follicles were not defined as follicles. The physician's evaluations and filtering results obtained from the applied methods were used to calculate the FRR and FAR using Equations (4) and (5), respectively.

$$FRR = \frac{FN}{TP+FN} \quad (4)$$

$$FAR = \frac{FP}{TN+TP} \quad (5)$$

3.3. Evaluation metrics for the segmentation

The evaluation criteria recommended in the literature were used to evaluate the success of the segmentation applied to images for automatic follicle detection. These parameters are the Dice score and Jaccard index.

3.4. Evaluation metrics for the classification results

The evaluation metrics suggested in literature were used to evaluate the classification success of the trained network. These are the accuracy, sensitivity, precision, and F1 scores.

4. RESULTS AND DISCUSSION

In this study, a dataset of 54 ovarian ultrasound images published publicly in 2021 was used, and various combinations of image processing techniques that worked best for USG images were compared. For this purpose, two different methods were developed for follicle detection in ovarian ultrasound images, and a total of 10 different algorithms were tested. The performances of the filters were compared by applying salt-and-pepper noise to the images.

A comparison of the results of the filtering and thresholding combinations tested in this study with the physician's evaluation is presented in Table 5, and the follicle detection accuracy and percentile FAR and FRR values are presented in Table 5. The performance evaluation of the filters is presented in Table 6 with the mean and standard deviation values. Among the filters, the Wiener filter provided the best result, with 0.02102 ± 0.0052 MSE and 65.0098 ± 1.0523 PSNR.

Table 5. Comparison of the proposed method with the physician evaluation and the follicle detection results (FP: Areas without follicles are perceived as follicles, FN: Areas with follicles are not perceived as follicles. FAR: False Acceptance Rate, FRR: False Rejection Rate

	Method	Number of Follicles (Physician Evaluation)	Number of Follicles (Proposed Method)	Correct Follicle Count	FP	FN	Follicle Detection Accuracy (%)	FAR (%)	FRR (%)
Standard thresholding	Median filter	381	541	182	359	199	47.76	66.35	36.78
	Mean filter	381	553	185	368	196	48.55	66.54	35.44
	Gaussian filter	381	624	225	399	156	59.05	63.94	25
	Wiener filter	381	561	178	383	203	46.71	68.27	36.18
Adaptive thresholding	Median filter	381	522	370	152	11	97.11	29.11	2.10
	Mean filter	381	68	368	200	13	96.58	35.21	2.28
	Gaussian filter	381	409	361	48	20	94.75	11.73	4.88
	Wiener filter	**381**	**559**	**372**	**187**	**9**	**97.63**	**33.45**	**1.61**
K-means clustering	Gaussian filter	381	522	320	202	61	83.98	38.6	11.68
	Discreate Wavelet Transform	381	531	319	212	62	83.72	39.92	11.67

Table 6. Performance evulation of the filters (Mean ± Standart Deviation)

	Median Filter	**Mean Filter**	**Gaussian Filter**	**Wiener Filter**	**DWT**
MSE	0.07122 ±0.0404	0.07936± 0.0485	0.0304± 0.0153	**0.02102± 0.0052**	0.0458± 0.0458
PSNR	60.1166 ±2.3053	59.7776± 2.6264	63.7697± 2.3083	**65.0098± 1.0523**	59.6069± 2.3723

As shown in Table 6, the highest follicle detection accuracy of 97.63% was obtained using the Wiener filter and adaptive thresholding. A median filter and adaptive thresholding are in second place with 97.11% accuracy, followed by a mean filter and adaptive thresholding, and a Gaussian filter and adaptive thresholding. Again, as can be seen from the tables, standard thresholding and histogram equalization show low results for all four filter types. When the tables were examined, although the Gaussian filter showed a good filtering performance, when combined with the contrast setting, the highest follicle recognition accuracy of 97.63% was obtained using the Wiener filter.

Fig.7 shows the outputs of the algorithms that provide the best results for both methods proposed in this study for automatic follicle detection. Dice score and Jaccard index parameters were used to evaluate the segmentation success. The highest automatic follicle detection success was achieved using adaptive thresholding with Wiener filter.

For this method, a 78.95% Dice Score and 65.66% Jaccard index were obtained; the results are given in Table 7.

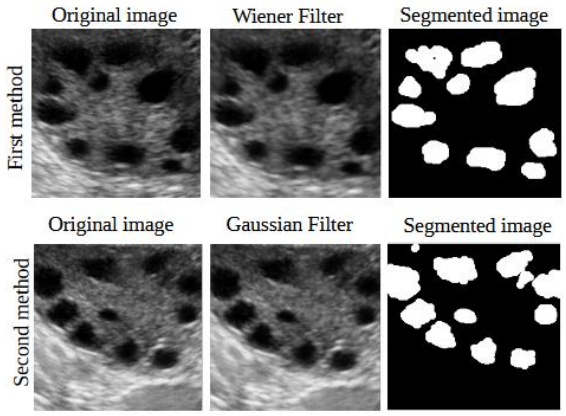

Fig.7. Segmented images for the first and second methods

Table 7. Performance evaluation of the segmentation

	First method: Wiener filter and adaptive thresholding
Dice Score	%78.95
Jaccard Index	%65.66

Segmented and unsegmented images were classified using a CNN in the next step of the study. Data augmentation was applied to increase the success of the convolutional neural network. The amount of data was increased fivefold with rotation, horizontal projection, vertical projection, and histogram thresholding. After follicle detection, the segmented images were recorded, and a new dataset was created. The neural network was trained using the recorded data, and ovarian ultrasound images were classified as “normal” and “pcos” For classification, the program was run ten times and each value was recorded, and the average results were evaluated. The classification results of the segmented and unsegmented images and the classification with transfer learning are presented in Table 8.

Table 8. Classification Results (%)

			Accuracy	**Sensivitiy**	**Precision**	**F1**
For unsegmented images	**CNN**	**Validation**	65.81	74.75	78.02	74.78
		Test	68.91	83.25	76.58	78.01
	SqueezeNet	**Validation**	74.18	67.07	69.33	68.164
		Test	70.48	65.02	63.42	64.30
For segmented images	**CNN**	**Validation**	77.81	94.45	79.53	76.21
		Test	72.36	90.25	86.22	82.60
	SqueezeNet	**Validation**	**75.54**	**78.82**	**57.1**	**64.83**
		Test	69.45	72.36	59.5	67.40

The approximate classification accuracy of the CNN trained with segmented images was 77.81% at 5 min and 4 s. The approximate classification accuracy of the CNN trained with unsegmented images was 65.81% at 5 min and 26 s. The network was first trained, and then the classification accuracies were tested with both the validation data and test data. The classification accuracy with test data in unsegmented images was 68.91% better than that of the validation data. However, in the segmented images, classification with validation data achieved a higher accuracy of 77.81% than the test data. The accuracy of classification using SqueezeNet-based transfer learning was 74.18 % for unsegmented images and 75.54 % for segmented images.

Sensivitiy, Precision, and F1 parameters were also used to evaluate the classification performance, as shown in Table 8.

When we searched the literature, we observed that there are a limited number of studies on follicle detection in ovarian images. The limited number of studies in this field have pointed to the conclusion that filter selection is important in denoising so that follicle detection can be performed with high accuracy. With this motivation we aimed this study in two different ways as both follicle detection with image processing and disease detection with deep learning. Among the filters applied in image processing, the Wiener filter provided the best filtering, with 0.02102±0.0052 MSE and 65.0098±1.0523 PSNR. Using the Wiener filter and adaptive thresholding, a high accuracy of 97.63% was achieved in determining the number of follicles. This situation reveals the importance of not only the selected filter, but also the thresholding process with the right combination in follicle detection. When we look at the studies that classify ovarian ultrasound images, we saw that classification is performed on unsegmented images in most studies, or the segmentation process is performed with CNN. In the classification phase of this study, applications were performed using both segmented and unsegmented images. After the neural network was trained with the training data, the classification success was compared with the validation and test data. In this study, the accuracy of the classification of segmented images was 77.81%. and a sensitivity of 94.45%. As an alternative to the proposed method, 74.18% success was achieved with transfer learning, which provided good results in limited datasets.

Wisesty et al. performed a follicle detection study using ten ovarian images. In this study. They compared the standard thresholding and Otsu Thresholding methods and calculated the number and diameter of follicles using an image segmentation and stereology approach with a Sobel filter. Otsu's Thresholding method provides better accuracy [43]. Adiwijaya et al. published a dataset containing 54 ovary images together with Wisesty [24]. In this study, follicle detection was performed with a dataset containing 54 images, and the number of data was increased to 270 with data augmentation techniques to be used in the classification phase. Wisesty et al. compared the results of their study using 10 ovarian images with those obtained using 54 ovary images in this study. An increase in the size of the dataset increases the accuracy of follicle detection[43]. In addition, the combination of the Wiener filter with adaptive thresholding has been successful in follicle detection for these images.

In the classification process, attention should be paid to two important situations: over-memorization and over-fitting. The risk of overfitting is relatively high if our model has started to memorize the dataset, we used it for training too much, or if the training set was monotonous. A database of 54 images was used in this study. Although the data were replicated using data-duplication techniques, they were small. A small amount of data and unbalanced dataset can cause overlearning. Therefore, to validate the results of the CNN structure proposed in this study, classification was performed using transfer learning, which is more suitable for small datasets.

The training and validation error curves (Fig8, Fig10 for our study) can be examined to determine whether a model has an over-learning problem. Overfitting may have occurred if the model had increased the errors in the validation set while reducing the errors in the training dataset. Sensitivity and precision values can also be considered for the training and validation data. Overfitting may occur if the model achieves high precision in the training dataset and has low values in the validation dataset. In our study, for segmented images the CNN model achieved an accuracy of 77.81%, a sensitivity of 94.45%, a precision of 79.53%, and an F1 score of 76.21%. On the other hand, transfer learning yielded similar results with an accuracy of 74.18%, a sensitivity of 67.07%, a precision of 69.33%, and an F1 score of 68.164%. Figure 9 and Figure 11 present the confusion matrices from which we obtained these results.

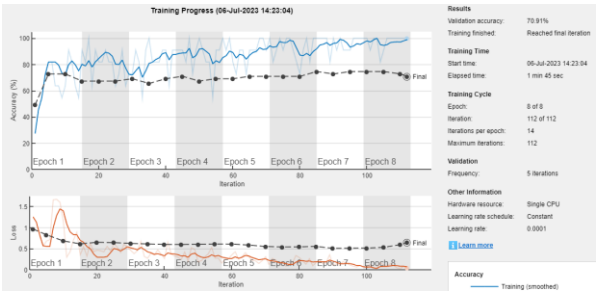

Fig.8. The accuracy graphic for SqueezeNet

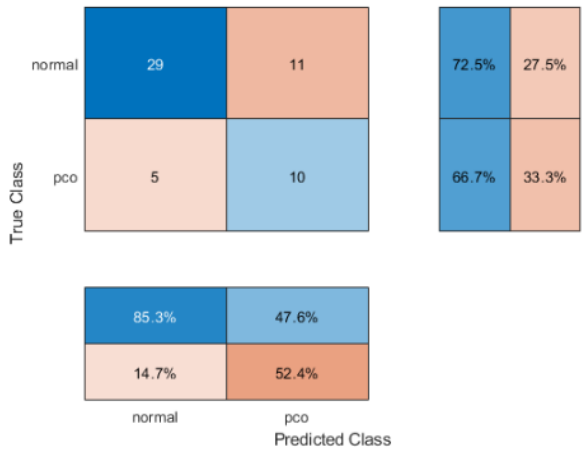

Fig.9. The confusion matrix for SqueezeNet

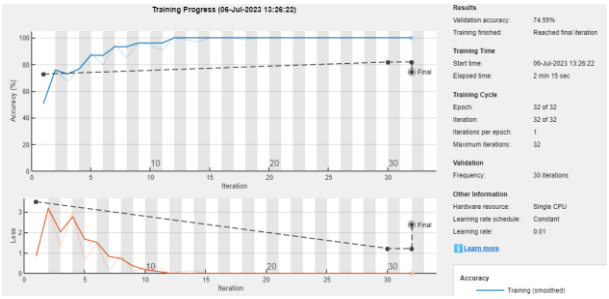

Fig.10. The accuracy graphic for proposed CNN

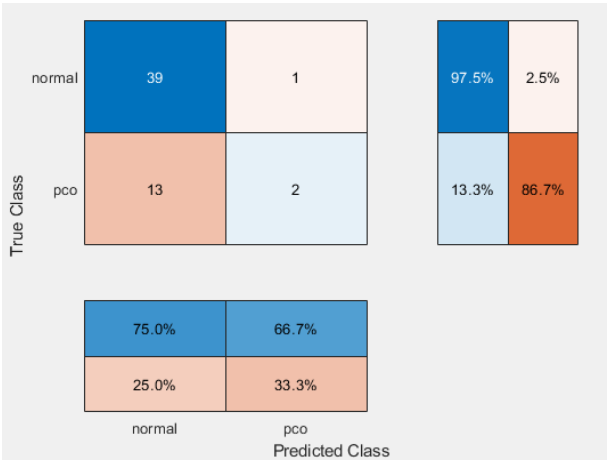

Fig.11. The confusion matrix for proposed CNN

6. CONCLUSION

PCOS is an important disease affecting the quality of life of many women. However, there is not enough data in the literature to investigate this disease and measure the success of follicle detection using image processing methods. Larger datasets can be created by recording ovarian images from hospitals to address the lack of data in the literature and ensure success in real-time applications of follicle detection and PCOS diagnosis in the ovaries. In addition, a decision-support system was designed.

In this study, a Convolutional Neural Network (CNN), which is a deep learning method, and SqueezeNet which uses transfer learning were preferred instead of machine-learning models. To test machine learning models, it is necessary to obtain the features that best represent the images using feature extraction techniques from preprocessed images. In this study, values such as the diameter of the follicles, their distance from each other, and the number of follicles can be considered as features to be extracted from the ovary images. On the other hand, deep learning models have features that can be preferred in automatic diagnosis systems by classifying unsegmented or segmented images without the need for a feature extraction process. For this reason, the ovary images we obtained for this study were limited to deep learning models, although data augmentation techniques were also applied. As a result, by using different deep learning architectures with more ovary images, the classification accuracy obtained in this study can be increased, and an automatic diagnosis system can be developed.

DECLARATION OF ETHICAL STANDARDS

The authors of this article declare that the materials and methods used in this study do not require ethical committee permission and/or legal-special permission.

AUTHORS' CONTRIBUTIONS

Perihan Gülşah GÜLHAN: Perofrmed the experiments, analyse the results and wrote the manuscript.

Güzin ÖZMEN: Perofrmed the experiments, analyse the results and wrote the manuscript.

Hüsnü ALPTEKİN: Analyse the results.

CONFLICT OF INTEREST

There is no conflict of interest in this study.

REFERENCES

[1] P. S. Hiremath and J. R. Tegnoor, "Follicle Detection and Ovarian Classification in Digital Ultrasound Images of Ovaries," in ***Advancements and Breakthroughs in Ultrasound Imaging***, Chapter 7: 167-197, (2013).

[2] A. Gougeon, "Dynamics of Human Follicular Growth: Morphologic, Dynamic, and Functional Aspects," ***The ovary,*** 2: 25-43, (2004).

[3] T. D. Pache, J. W. Wladimiroff, W. C. Hop, and B. C. Fauser, "How to discriminate between normal and polycystic ovaries: transvaginal US study.," ***Radiology,*** 183.2:421–423, (1992).

[4] E. S. Knochenhauer, T. J. Key, M. Kahsar-Miller, W. Waggoner, L. R. Boots, and R. Azziz, "Prevalence of the Polycystic Ovary Syndrome in Unselected Black and White Women of the Southeastern United States: A Prospective Study1," ***J Clin Endocrinol Metab***, 83(9):3078–3082, (1998).

[5] T. R. ESHRE and A.-S. P. C. W. Group, "Revised 2003 consensus on diagnostic criteria and long-term health

[7] S. M. Pfeifer, "Polycystic ovary syndrome in adolescent girls," ***Semin Pediatr Surg***, 14(2):111–117, (2005).

[8] D. E. Lane, "Polycystic Ovary Syndrome and Its Differential Diagnosis," ***Obstet Gynecol Surv,*** 61.2:125-135, (2006).

[9] A. Dunaif, M. J. Graf, J. P. Mandeli, V. Laumas, and A. Dobrjansky, "Characterization of groups of hyperandrogenic women with acanthosis nigricans, impaired glucose tolerance, and/or hyperinsulinemia.," ***J Clin Endocrinol Metab***, 65(3):499–507, (1987).

[10] A. Gougeon and B. Lefèvre, "Evolution of the diameters of the largest healthy and atretic follicles during the human menstrual cycle," ***Reproduction***, 69(2):497–502, (1983).

[11] C. Battaglia *et al.*, "Color Doppler analysis in oligo-and amenorrheic women with polycystic ovary syndrome," ***Gynecological Endocrinology***, 11(2):105–110, (1997).

[12] A. H. Balen, J. S. E. Laven, S. Tan, and D. Dewailly, "Ultrasound assessment of the polycystic ovary: international consensus definitions," ***Hum Reprod Update***, 9(6):505–514, (2003).

[13] M. J. Lawrence, M. G. Eramian, R. A. Pierson, and E. Neufeld, "Computer Assisted Detection of Polycystic Ovary Morphology in Ultrasound Images," **in *Fourth Canadian Conference on Computer and Robot Vision***, CRV '07: 105–112, (2007).

[14] P. Hiremath and J. Tegnoor, "Automatic Detection of Follicles in Ultrasound Images of Ovaries using Edge Based Method," ***IJCA, Special Issue on RTIPPR 2***, 120-125, (2010).

[15] B. Purnama, U. N. Wisesti, Adiwijaya, F. Nhita, A. Gayatri, and T. Mutiah, "A classification of polycystic Ovary Syndrome based on follicle detection of ultrasound images," in ***2015 3rd International Conference on Information and Communication Technology (ICoICT),*** 396–401, (2015).

[16] U. N. Wisesty, "Implementasi Gabor Wavelet dan Support Vector Machine pada Deteksi Polycystic Ovary (PCO) Berdasarkan Citra Ultrasonografi," ***Indonesia Journal on Computing (Indo-JC),*** 1(2):67–82, (2016).

[17] B. Padmapriya and T. Kesavamurthy, "Detection of follicles in poly cystic ovarian syndrome in ultrasound images using morphological operations," ***Journal of Medical Imaging and Health Informatics***, 6(1):240–243, (2016).

[18] C. Sonigo *et al.*, "High-throughput ovarian follicle counting by an innovative deep learning approach," ***Scientific Reports***, 8(1):13499, (2018).

[19] A. Nazarudin, N. Zulkarnain, A. Hussain, S. Mokri, and I. N. A. Mohd Nordin, "Review on automated follicle identification for polycystic ovarian syndrome," ***Bulletin of Electrical Engineering and Informatics***, 9(2):588-593, (2020).

risks related to polycystic ovary syndrome," ***Fertil Steril***, 19(1):19–25, (2004).

[6] F. J. M. Broekmans, E. Knauff, O. Valkenburg, J. Laven, M. Eijkemans, and B. Fauser, "PCOS according to the Rotterdam consensus criteria: Change in prevalence among WHO-II anovulation and association with metabolic factors", ***BJOG: An International Journal of Obstetrics & Gynaecology,*** 113(10):1210-1217, (2006).

[20] T. Zeng and J. Liu, "Automatic detection of follicle ultrasound images based on improved Faster R-CNN," ***J Phys Conf Ser,*** 1187(4):042112, (2019).

[21] M. Jayanthi Rao and R. Kiran Kumar, "Follicle Detection in Digital Ultrasound Images Using BEMD and Adaptive Clustering Algorithms," in ***Innovative Product Design and Intelligent Manufacturing Systems***: Select Proceedings of ICIPDIMS 2019, 651–659, (2020).

[22] Ö. İnik, A. Ceyhan, E. Balcıoğlu, and E. Ülker, "A new method for automatic counting of ovarian follicles on whole slide histological images based on convolutional neural network," ***Comput Biol Med,*** 112:103350, (2019).

[23] B. Rachana, T. Priyanka, K. N. Sahana, T. R. Supritha, B. D. Parameshachari, and R. Sunitha, "Detection of polycystic ovarian syndrome using follicle recognition technique," ***Global Transitions Proceedings,*** 2(2):304–308, (2021).

[24] Adiwijaya, U. NOVIA WISESTY, and W. Astuti, "Polycystic Ovary Ultrasound Images Dataset." **Telkom University Dataverse**, (2021).

[25] P. G. YILMAZ and G. ÖZMEN, "Follicle Detection for Polycystic Ovary Syndrome by using Image Processing Methods," ***International Journal of Applied Mathematics Electronics and Computers***, 8(4):203–208, (2020).

[26] R. C. Gonzalez, "Digital image processing", ***Pearson education india***, (2009).

[27] Y. Zhu and C. Huang, "An improved median filtering algorithm for image noise reduction," ***Phys Procedia***, 25:609–616, (2012).

[28] J. W. Tukey, "Exploratory data analysis", 2: 131-160, (1977).

[29] W. K. Pratt, Digital image processing: PIKS Scientific inside, ***Hoboken, New Jersey: Wiley-interscience***, Vol.4, (2007).

[30] M. M. P. Petrou and C. Petrou, "Image processing: the Fundamentals", ***John Wiley & Sons***, (2010).

[31] P. Soille, "Morphological image analysis: principles and applications", ***Springer***, 2(3): 170-171, (1999).

[32] N. Efford, "Digital image processing: a practical introduction using java (with CD-ROM)", **Addison-Wesley Longman Publishing**, (2000).

[33] N. I. Chervyakov, P. A. Lyakhov, and N. N. Nagornov, "Quantization noise of multilevel discrete wavelet transform filters in image processing," ***Optoelectronics, Instrumentation and Data Processing,*** 54:608–616, (2018).

[34] V. Kiruthika and M. M. Ramya, "Automatic segmentation of ovarian follicle using K-means clustering," in ***2014 fifth international conference on signal and image processing***, 137–141, (2014).

[35] B. Brahmadesam Viswanathan Krıshna, "Image pattern recognition technique for the classification of multiple power quality disturbances," ***Journal of Electrical and Computer Sciences,*** 21(3):656–678, (2013)

[36] G. Gupta, "Algorithm for image processing using improved median filter and comparison of mean, median and improved median filter," ***International Journal of Soft Computing and Engineering (IJSCE),*** 1(5):304–311, (2011).

[37] S. S. Khan and A. Ahmad, "Cluster center initialization algorithm for K-means clustering," ***Pattern Recognit Lett,*** 25(11):1293–1302, (2004).

[38] T. Brosnan and D.-W. Sun, "Improving quality inspection of food products by computer vision—a review," ***Journal of Food Engineering,*** 61(1):3–16, (2004).

[39] J. Schmidhuber, "Deep learning in neural networks: An overview," ***Neural networks***, 61:85–117, (2015).

[40] W. You, C. Shen, D. Wang, L. Chen, X. Jiang, and Z. Zhu, "An intelligent deep feature learning method with improved activation functions for machine fault diagnosis," ***IEEE Access***, 8:1975–1985, (2019).

[41] S. Minaee, R. Kafieh, M. Sonka, S. Yazdani, and G. J. Soufi, "Deep-COVID: Predicting COVID-19 from chest X-ray images using deep transfer learning," ***Medical Image Analysis,*** 64:101794, (2020).

[42] A. Hore and D. Ziou, "Image quality metrics: PSNR vs. SSIM," ***in 2010 20th international conference on pattern recognition,*** **IEEE,** 2366–2369, (2010).

[43] I. F. Thufailah and U. N. Wisesty, "An implementation of Elman neural network for polycystic ovary classification based on ultrasound images," in ***Journal of Physics: Conference Series,*** 971(1):120168, (2018).